ACS APPLIED MATERIALS & INTERFACES

Research Article

www.acsami.org

Manipulation of Polymer/Polymer Interface Width from Nonequilibrium Deposition

Wumin Yu,[†] Someswara R. Peri,[†] Bulent Akgun,[‡,§,⊥] and Mark D. Foster*[,†]

[†]Department of Polymer Science, The University of Akron, Akron, 170 University Avenue, Akron, Ohio 44325-3909, United States
[‡]NIST Center for Neutron Research, National Institute of Standard and Technology, Gaithersburg, Maryland 20899, United States
[§]Department of Materials Scence and Engineering, University of Maryland, College Park, Maryland 20742, United States

Supporting Information

ABSTRACT: We demonstrate, using neutron reflectivity, that the width of a nonequilibrium interface between an organo-soluble aromatic polyimide film and triacetate cellulose (TAC) support film created by spin-coating or solution-casting can be broadened in a controllable way using a "swelling agent" in the deposition process. In a favorable case, the adhesion, as measured by T-peel tests, can be increased by a factor of 7 by adjustment of the solvent composition. The morphologies of the TAC fractured surfaces after peeling tests measured by AFM reveal that broadening of the interfacial width causes an interconnected network in the interface, leading to a sharp increase in the interfacial adhesion. Differences in the chemistry (solubility) of the materials being deposited do make a difference in the effectiveness of this strategy of using a "swelling agent". For one polyimide, a 3-fold increase in adhesion can be obtained by optimizing the deposition temperature, but this approach for improving adhesion is less effective than that of adding "swelling agent". The formation of robust interfaces of this type is important because of the critical roles that multilayer films containing polymers with special properties and tailored structures play in applications as diverse as computer displays, photovoltaic devices, and polymeric electronics. The "swelling agent" strategy makes it possible to produce polymer multilayer structures in a cost-effective way with roll-to-roll mass production using direct solution coating.

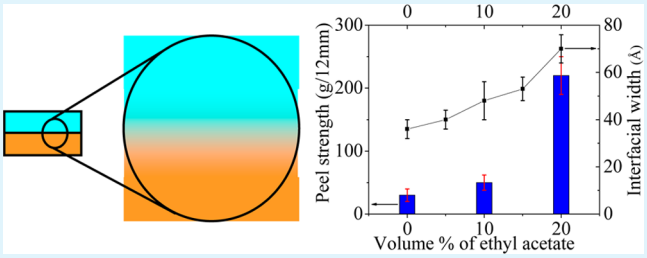

KEYWORDS: *solution coating, polyimide, polymer interface, peel test, neutron reflectivity, fracture surface*

1. INTRODUCTION

Multilayer films of diverse polymers are attracting fundamental and industrial interest due to the wide range of applications for such films. Due to its low cost and suitability for mass production, solution casting is still the preferred method for depositing these multilayers. For reliability of devices containing multilayer polymer films, the adhesion between pairs of polymer layers is important. However, generally using solution casting requires that the solvent for depositing one polymer not significantly swell or dissolve the underlying polymer layer.[1] Often the polymers used in these multilayers are also highly immiscible. This designed lack of solubility and the intrinsic immiscibility between polymers limit the mutual penetration of the two polymer layers during deposition, usually leading to a weak interface. To improve the reliability and lifetime of the devices containing multilayer polymer films, sufficient interfacial adhesion is required to withstand the stresses developed during processing and operation.[2,3] The objective of this research was to understand the interfacial structure formed by solution casting and the opportunities for optimizing the coating parameters to achieve better interlayer adhesion.

A key means of creating an interface able to withstand all kinds of stresses developed during processing and device operation is to achieve substantial interdiffusion of the two polymers at the interface. There have been many studies[4−16] of the structure of model polymer/polymer interfaces at thermodynamic equilibrium where detailed comparisons can be made with predictive theories developed by Helfand and co-workers[17−19] based on first principles. Also the connection between adhesion and interface width for these equilibrium interfaces has been probed by several authors.[8,9,11,15] All of these studies show that entanglements are the primary sources of adhesion and the adhesive strength is directly correlated with the interfacial width. Nonequilibrium interfaces are more complicated than their equilibrium analogs, but are common in practice. One particular example is that of the interface between polyimide films used as compensation layers and the films used for their support in liquid crystal displays (LCDs) deposited by direct solution casting.[1] Rigid rodlike aromatic polyimides (PIs) show uniaxial negative birefringence and have

Received: October 8, 2012
Accepted: March 4, 2013
Published: April 5, 2013

dx.doi.org/10.1021/am3022587 | ACS Appl. Mater. Interfaces 2013, 5, 2976−2984

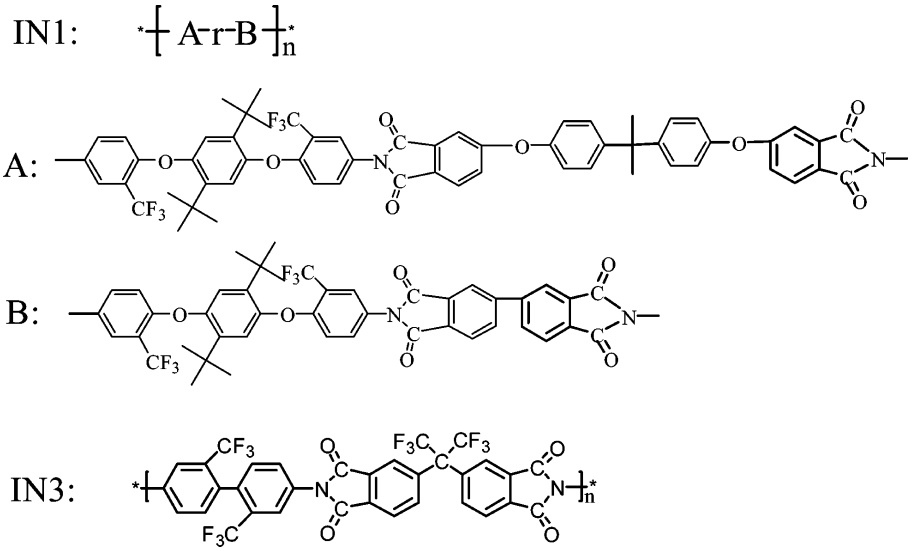

Figure 1. Chemical structure of IN1 and IN3. A-*r*-B in IN1 represents a random distribution of A and B units in the molecules.

been used as compensation films to widen the viewing angles of LCDs.[1,20] Here we consider specifically PI copolymers that are soluble in common organic solvents and therefore suitable for solution casting.[21−23]

The conventional process to deposit a compensation film for incorporation into a LCD system is a multistep process.[1] The PI is first cast from solution onto a carrier substrate. Then adhesive is applied to the PI surface. The carrier is finally removed after the PI film with adhesive is laminated on a LCD component. To simplify the deposition process and reduce cost, those in industry prefer solution-casting the PI film directly on a substrate film, e.g. triacetate cellulose (TAC).[1] To obtain high-quality multilayer films with excellent durability, sufficient interlayer adhesion is needed. However, this solution casting process does not readily form interfaces with good adhesion, because of the use of nonsolvent (for the TAC) for the coating process and the high immiscibility between PI and TAC. Here we have focused on understanding this particular solution casting process by probing the buried interface as deposited and how deposition conditions affect adhesion. This approach could be applied to other immiscible polymer/polymer interfaces of commercial relevance.[24−26]

Neutron reflectivity (NR) has been used to determine the polymer/polymer interface structure because it offers an extraordinary depth resolution of 10 Å.[27,28] NR is sensitive to gradients in the neutron scattering length density, (b/V), in the direction perpendicular to the film surfaces, with

$$(b/V) = \frac{N_A \rho b_{mon}}{M_{mon}} \quad (1)$$

where N_A is Avogadro's number, ρ is the mass density of the polymer, b_{mon} and M_{mon} are the sum of scattering lengths and the molar mass of the repeating monomer unit, respectively. Probing the structure of an interface with NR requires contrast, or a difference in scattering length densities, between the two polymer layers. In this work the PI fluorine content provides contrast between a PI layer and a TAC layer without needing deuterium labeling.

The focus of this work was to understand how introducing a minority fraction of a second solvent into the casting solution or adjusting the temperature can be used to modify the interface structure. This second solvent, which is able to swell the TAC somewhat, but not dissolve it, we refer to as a "swelling agent". It is shown that the interface width and thus the interlayer adhesion between PI and TAC can be significantly increased by adding swelling agent, although the effectiveness of the swelling agent is highly dependent on the properties of the PI. We also demonstrate that the interfacial width and adhesion can be increased by optimizing the coating temperature, but varying temperature is less efficient than using a swelling agent due to the accumulation of larger residual stresses at higher coating temperature.

2. EXPERIMENTAL SECTION

Materials. Two soluble polyimide samples, IN1 and IN3, for which the chemical structures are shown in Figure 1, were synthesized by Akron Polymer Systems, Inc. using a one-step polymerization method.[29] IN1, which has a fluorine content of 12.5 at. wt% was synthesized from 2,2′-*bis*[4-(3,4-dicarboxyphenoxy)phenyl]propane dianhydride (BisADA), 4,4′,5,5′-biphenyltetracarboxylic dianhydride (BPDA) and 1,4-*bis*(2-trifluoromethyl-4-aminophenoxy)-2,5-di-(tbutyl)benzene (BTBDA) using a molar ratio of 1:1:2. IN3, which has a fluorine content of 31.3 at. wt% was prepared by polymerizing 2,2′-bis(3,4-dicarboxyphenyl)hexafluoropropane dianhydride (6FDA) and 2,2′-(trifluoromethyl)-4,4′-diaminobiphenyl diamine (PFMB). Molecular weights of IN1 and IN3 were obtained using gel permeation chromatography in THF with polystyrene standards are listed in Table 1. LCD grade cellulose triacetate (TAC, CA-436−45S) was provided by Eastman Chemical Company. The bulk glass transition temperatures of the polyimides and TAC were determined by differential scanning calorimetry (DSC) using a heating rate of 10 °C/minute and taking data from the second heating scan (Data for TAC and IN1 in Supporting Information, Figures S1,S2) .

Table 1. Molecular Weights of Polyimide Samples

PI	F content at wt %[a]	polystyrene equivalent M_w[b] (g/mol)	$M_w/M_n \pm 10\%$	T_g (°C)
IN1	12.5	1.0×10^5	2.4	247[c]
IN3	31.3	1.4×10^5	3.4	344[c,d]

[a]Calculated on the basis of the monomer composition in the feed, ± 0.2 wt %. [b]Determined by GPC in THF at 30 °C with polystyrene standards, ± 10%. [c]Determined using DSC on second heating scan, ± 5 °C. [d]From Li et al.[30]

Sample Preparation. Samples for either NR or T-peel tests were deposited on 3 in. diameter silicon wafer substrates. The silicon wafers were first cleaned in a piranha solution (a 3:1 mixture of concentrated sulfuric acid with 30% hydrogen peroxide[31]) at 90 °C for 30 min to remove organic residue. After being rinsed with copious amounts of pure (18 MΩ) water, the silicon wafers were immersed in a 1% hydrofluoric acid solution in water for 1 min to etch off the silicon oxide, then rinsed with DI water and blown dry with nitrogen gas. To obtain reproducible sample structure and behavior the silicon oxide was regrown in a clean desiccator over 48 h. Samples for NR measurements were prepared by first spin-coating a smooth TAC layer with a thickness of about 45 nm on a clean silicon substrate. The TAC coating solution was prepared by dissolving 0.06 g TAC in 10 mL of a solvent mixture of acetic acid and dichloromethane in a volume ratio of 7:3 and then filtering three times with a 0.45 μm filter before coating. The PI layer was deposited using two different methods, spin coating or solution casting, to deposit a layer of about 40 nm thick on top of a TAC layer to form a bilayer structure. To prepare bilayer samples with high quality using solution casting, a leveled tripod table was used. PI was dissolved in methyl isobutyl ketone (MIBK) to form the coating PI solution. The PI solution was allowed to drop on top of the TAC layer and spread and then the table was covered, leaving a small gap to allow evaporation of the solvent. The size of the gap controlled the evaporation rate. The tripod table could be heated under feedback control to perform solution casting at temperatures above ambient. The bilayer samples were further dried in a roughing vacuum oven (with LN_2 trap) at 130 °C for 48 h to remove residual solvent before NR measurements. Since the T_g of TAC was measured by DSC to be 180 ± 4 °C, we anticipate there was no interdiffusion during the process of removing residual solvent. Bilayer samples for T-peel tests were prepared by sequential solution casting of TAC and PI using the same setup as used in preparing NR samples. Higher solution concentrations were used to form a TAC layer with thickness of about 0.06 mm and PI layer with thickness about 0.02 mm. Each bilayer sample was peeled off its substrate and cut into 60 mm × 12 mm strips for T-peel tests. For each set of coating parameters, at least three samples were prepared and tested.

NR Measurements. NR measurements were performed at the National Institute of Standards and Technology (NIST) Center for Neutron Research on the NG7 horizontal reflectometer using a neutron beam of wavelength 0.475 nm and 35 mm width. The wavelength spread ($\Delta\lambda/\lambda$) was about 0.02. To maximize the intensity, the sizes of the collimating slits and detector slits were increased during the measurement as the incident angle increased, keeping the relative resolution ($\Delta q/q$) at an approximately constant value of 0.04.

T-peel Test Measurements. T-peel tests were carried out on a TA Instruments RSA3 Dynamic Mechanical Analyzer (DMA) at room temperature. The peeling speed was 0.3 mm/second. Data were collected as normal force versus time.

3. RESULTS AND DISCUSSION

For an equilibrium interface between two immiscible, flexible polymers, the interface width is determined by their thermodynamic incompatibility and the chain segment sizes. In the limit of large molecular weights the equilibrium interface width can be predicted using the mean field theory of Helfand and Tagami.[17] However, in the direct coating process, interdiffusion of the polymer molecules across the interface is generally possible only before the solvent has evaporated. Because of the finite time available for the interface to form, the interface is determined by both the thermodynamics and the dynamics of the chains.

To better understand the direct coating process, we first look at the interface formed at the very early stages of interdiffusion. This regime is important because the onset of interfacial strength development will take place during these early stages.[32] Casting bilayers using spin coating allows us to probe film formation in the case of quite short casting times. Spin-coating also provides films of very good thickness uniformity and low microroughness, which are ideally suited to study with NR. Both NR and X-ray reflectivity measurements (see the Supporting Information, Figures S3 and S4) of TAC films onto which PI films were cast showed them to be very uniform in scattering length density through the film. Surface microroughnesses measured by X-ray reflectivity were about 0.7 nm rms. Figure 2 shows the NR data and best model

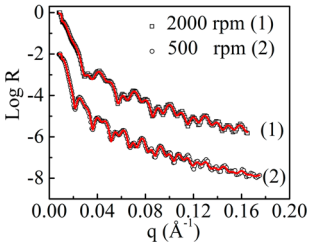

Figure 2. NR data (symbols) and best-fits (solid lines) for IN3/TAC bilayer films deposited by spin coating the PI from MIBK solution on top of a TAC layer at spin coating speeds of (1) 2000 and (2) 500 rpm, respectively. The reflectivity curves have been shifted vertically for clarity.

fits for the bilayer IN3/TAC films prepared by spin coating the PI in MIBK solution on top of the TAC layer using different rotational velocities. The reflectivity curves look quite different because the thicknesses of both the TAC and PI layers differ between the samples. The NR curves were fit with the assistance of the software package REFLPAK[33] to generate real space scattering length density (SLD) profiles. A two-layer model consisting of a PI layer and a TAC layer on top of a silicon wafer with its native silicon oxide was used to fit the data. The portions of the SLD profiles including the PI/TAC interfaces are shown in Figure 3 and the entire SLD profile and

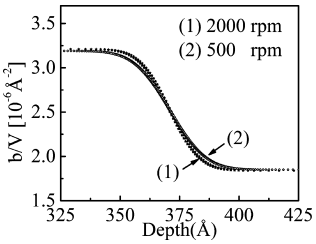

Figure 3. SLD profiles for samples for which NR data are shown in Figure 2. For clarity, only the parts of the SLD profiles near the PI/TAC interfaces are shown.

detail for the PI/air interfaces are shown in Supporting Information (Figures S5, S6). The interfacial width between the PI and TAC layers was modeled by an error function, with the width expressed as the full width at half-maximum (fwhm). The b/V values for TAC and IN3 obtained from fitting the data were (1.80 ± 0.05) × 10^{-6} and (3.20 ± 0.05) × 10^{-6} Å^{-2}, respectively. The b/V value for TAC agrees well with a value calculated assuming a mass density of 1.3 g/cm^3 from Omatete et al.[34] and Mulder et al.[35] The thickness of the native oxide layer was 1.1 ± 0.2 nm with a surface RMS roughness in the range of 0.3 to 0.5 nm. The TAC films were 42.0 ± 0.2 nm and 46.3 ± 0.2 nm in thickness and the PI films spun at 2000 and 500 rpm had thicknesses of 21.8 ± 0.2 nm and 36.7 ± 0.2 nm, respectively. In addition, the PI film spun at 500 rpm was somewhat rougher, with an RMS roughness of 0.6 ± 0.1 nm,

whereas the RMS roughness of the PI film spun at 2000 rpm was 0.4 ± 0.1 nm.

The apparent width of the polymer/polymer interface between TAC and PI, which includes the intrinsic width, the microroughness, and the effect of any capillary waves[36−38] at the interface is notably larger than the apparent width of the TAC/air interface. The RMS roughness of the TAC layer measured by both NR and AFM before addition of the PI layer was 0.7 ± 0.1 nm (which would correspond to a laterally averaged interface width of 1.6 nm fwhm). (The fwhm value is calculated from the RMS roughness by multiplying by $(2\pi)^{1/2}$.[37]) The PI/TAC apparent interface width is 2.3 ± 0.2 nm fwhm for the sample spun at 2000 rpm, so the difference between the TAC/air interface width and the PI/TAC interface width is 0.7 ± 0.2 nm fwhm. This increase is less than that seen by Fujii et al.,[39] (2.1 nm fwhm) who spun cast a polystyrene (PS) film (M_n = 54k) directly onto a layer of poly(methyl methacrylate) (PMMA) (M_n = 49k) using cyclohexane, which was a poor solvent for PS and a nonsolvent for the PMMA.[40] However, their resulting interface width of 2.6 nm fwhm was quite similar to the interface width after spin-casting seen here.

The solution is in contact with the TAC film surface for 2−3 s before the spinning starts, and then, for the case of 2000 rpm spin speed, changes in thickness due to loss of solvent are seen for 3−4 s (until the film color stops changing), so the total time for interdiffusion to occur before most of the MIBK solvent has evaporated, and the mobility necessary for interdiffusion is gone, is 5−7 s. When the spinning speed is decreased to 500 rpm, the contact time during which interdiffusion can occur increases to 14−16 s. Even though the contact time increases by more than a factor of 2, the increase in apparent polymer/polymer interface width, to 2.5 ± 0.3 nm fwhm, is within the experimental uncertainty. An additional 9 s of contact with the casting solution (for the 500 rpm case) makes little difference in the polymer/polymer interface width.

The interface width measured by NR (data, fit, and SLD profile shown in the Supporting Information, Figures S7, S8) for the bilayer sample created by spin-casting a solution of IN1 in MIBK on a TAC film is even smaller than that seen for IN3 on TAC. The interface width for IN1 spun cast at 2000 rpm is 1.8 ± 0.2 nm. This smaller interface width is consistent with the greater immiscibility of IN1 with TAC (discussed below).

We conjecture that the nonequilibrium interface width created by the spin-casting process is limited by a step in which the TAC surface is first plasticized so that interdiffusion can occur. In theorizing about polymer dissolution, Ueberreiter and co-workers[41−43] suggested that the dissolution of a polymer in a good solvent involves the formation of a swollen surface layer and summarized the structure of glassy polymers during dissolution from the pure polymer to the pure solvent as consisting of four layers. These four layers, listed beginning from the glassy polymer side are: an infiltration layer, a solid swollen layer, a gel layer, and a liquid layer. It is possible that even when a poor solvent or nonsolvent is placed on the glassy polymer, as in our case, there might exist a highly mobile surface layer (similar to the liquid layer in Ueberreiter's model) which allows the rapid intermixing of PI and TAC polymers across the interface during direct coating.

The process of interface formation in direct coating is a complicated one. As a first approximation we separate it into two component processes. First, there has to be solvent diffusion into the bottom layer and swelling of the polymer in that bottom layer to attain some degree of mobility to allow interdiffusion. The second process is polymer mutual diffusion between the layers, which can only involve this mobile region. A hypothesis on which this work was based was that interfacial adhesion, and therefore durability of the interface (and the device), could be improved by achieving a broader interface when depositing the PI layer.[8,11] If molecular mobility of a top layer of the TAC film during the brief coating process is key to good interdiffusion, addition of a solvent that could rapidly plasticize and swell the TAC film surface should be helpful. To investigate the ability of a "swelling agent" to provide this very rapid plasticization, ethyl acetate was added to the polyimide IN3 in MIBK coating solution and bilayers were formed using spin coating. The NR curves and fits for those data are shown in Supporting Information (Figures S9, S10). As shown in Figure 4, the interfacial width increases monotonically with

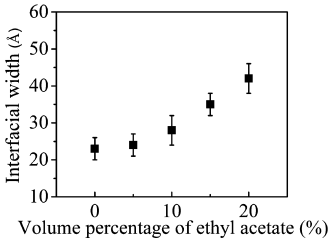

Figure 4. Interfacial widths of IN3/TAC bilayer films as a function of volume percentage of swelling agent ethyl acetate for films deposited by spin coating at 2000 rpm and then drying at 130 °C in a roughing vacuum oven for 24 h. The error bars in this figure and in the rest of the text represent ±1σ.

increasing volume percentage of ethyl acetate in the polyimide coating solution over the range of 0−20 vol %. Even when the time available for diffusion during deposition is very short (as it is in spin-casting), the interfacial width is adjustable using a swelling agent. Apparently, the addition of ethyl acetate to the coating solution enhances the mobility of the TAC surface layer, despite the fact that ethyl acetate is a poor solvent for the TAC layer.

The effect of a swelling agent on the interface formation process can also be considered for a slower deposition process based on solution casting. We look first at the interface formation without swelling agent. When the upper PI film is cast on the TAC substrate using conventional solution casting, 1.5 h are required for the majority of the MIBK solvent to evaporate from the film. Figure 5 compares the SLD profiles (NR data and fits shown in Supporting Information, Figure S11) for two IN3/TAC bilayer films, one prepared by spin coating and the other by solution casting. The fwhm interface

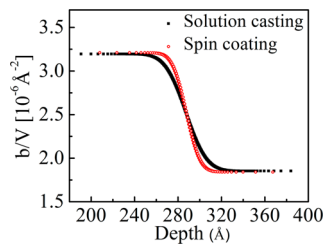

Figure 5. Comparison of the interface SLD profiles of two IN3/TAC bilayer films, one deposited from MIBK solution by spin coating at 2000 rpm (open circles), and the other by solution casting (solid squares).

dx.doi.org/10.1021/am3022587 | ACS Appl. Mater. Interfaces 2013, 5, 2976−2984

widths are 2.3 ± 0.2 nm by spin coating and 3.6 ± 0.4 nm by solution casting, a difference of 1.3 nm (ca. 50%) for these two cases in which the times available for polymer diffusion differ dramatically (5 s vs >5400 s). We note that for IN1 the fwhm interface widths from spin-coating and solution-casting are 1.8 ± 0.2 nm and 3.1 ± 0.3 nm, respectively. The absolute difference (1.3 nm) is the same as for the IN3.

The swelling agent ethyl acetate was added to solutions of IN3 in MIBK to prepare by direct solution casting bilayer samples with broader interfaces that should provide better adhesion. The broadening of interface with addition of ethyl acetate is shown in Figure 6 (NR data, fits, and SLD profile shown in the Supporting Information, Figures S12 and S13). The interfacial width between IN3 and TAC can be controlled by varying the volume fraction of ethyl acetate in both depositions with short diffusion times (spin coating) and long diffusion times (solution casting). The larger uncertainties in the interface widths in Figure 6 are due to the difficulty in controlling the thickness uniformity across the film for the case of direct solution casting. The data in Figure 6 also demonstrate that up to a factor of 2 increase in interfacial width can be achieved by adding up to 20 vol % ethyl acetate. Now the question is how much the broadening in interfacial width increases the interlayer adhesion.

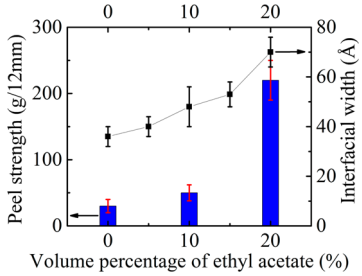

Figure 6. Comparison of the variations in peel strength and interfacial width with volume fraction of swelling agent ethyl acetate for IN3/TAC bilayer films prepared by solution casting. Interface widths measured with NR are shown with symbols and read from the right vertical axis. The line is a guide to the eye. Peel strengths shown with solid bars correspond to the left vertical axis. Peel strength increases sharply with increasing interface width in this regime.

The effect on interlayer adhesion was ascertained using T-peel tests using films much thinner than those used conventionally for peel tests, but still much thicker than the layers studied with reflectivity. The TAC films were about 60 μm thick and the PI films about 20 μm thick. IN3/TAC bilayer samples were prepared by solution casting using 0, 10, or 20 vol % ethyl acetate. The peel test results in Figure 6 show a sharp increase in peel strength with an increase in the volume fraction of ethyl acetate from 10 to 20 vol %.

To explain the sharp increase in peel strength we consider work done by others on the mechanisms by which polymer/polymer interfaces fail. It has been reported that when entanglements are the main source of adhesion (i.e., no specific chemical interactions), the adhesive failure process can involve three mechanisms: chain pullout, chain scission or crazing. The dominant mechanism depends on the interfacial width.[8,11] For small interfacial widths the adhesion strength is low and fracture energy is mainly dissipated through chain pullout or chain scission. At intermediate values of interfacial width these authors have seen the adhesion strength increase rapidly over a small range of interfacial widths due to the development of a plastic zone and there is a transition from chain scission or chain pullout to crazing. For sufficiently large interfacial widths, many entanglements across the interface are established and the adhesion strength reaches its bulk value and does not change further with interfacial width. We surmise that the sharp change in strength in going from 10% to 20% swelling agent is due to a change in failure mechanism from chain scission or chain pullout to crazing. None of our data correspond to the plateau region in which adhesive strength is independent of interface width.

Some additional information about how the character of the failure varied with percentage of swelling agent used was obtained by imaging the fracture surfaces with AFM. The textures and microroughnesses of the fracture surfaces changed much less between 0 and 10 vol % than they did between 10 and 20 vol %, as shown in the plot of microroughness vs vol % swelling agent shown in Supporting Information (Figure S14). The microroughnesses for 0 and 10 vol % were 3.4 and 8.7 nm RMS, respectively, while that for 20 vol % was 27.0 nm RMS. We conjecture that these roughnesses reflect contributions from the solution casting of the TAC film (which will yield rougher surfaces than can be achieved with spin-coating), solution casting of the PI on top of the TAC film, and from the fracture process itself. The texture of the fracture surface for the 20 vol % sample was also characterized by the presence of many sharp "spikes", while the fracture surface features for the 0 and 10 vol % samples were more rounded. These sharp "spikes" suggest the existence of connection points between TAC and IN3 before debonding. We attribute formation of the connection points to formation of entanglements across the interface for that level of swelling agent.

The polyimide IN1was also studied to test how the change in chemical structure affects the "swelling agent" strategy to broaden the interfacial width. The main difference in chemical structures between IN1 and IN3 is the fluorine content. As noted in Table 1, although IN3 contains 31.3 wt % fluorine, IN1 contains only 12.5 wt %. As shown in Figure 7, a very sharp interface was formed by IN1 with TAC and the interfacial width did not change on an experimentally significant level when the volume fraction of swelling agent in the casting solution was increased up to 20 vol %. The peel strengths shown in Figure 7 are likewise unchanging with swelling agent vol %, consistent with the lack of change in interfacial width.

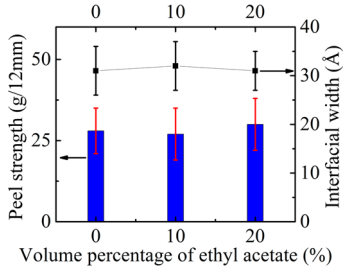

Figure 7. Comparison of the variations in peel strength and interfacial width with volume fraction of swelling agent ethyl acetate in the casting solution for IN1/TAC bilayer films prepared by solution casting. Interface widths measured with NR are shown with symbols and read from the right vertical axis (NR data, fits and SLD profile in Supporting Information, Figures S15 and S16). The line is a guide to the eye. Peel strengths shown with solid bars correspond to the left vertical axis.

To explain why these two polyimides behaved so differently with the "swelling agent" strategy, we first estimate the character of the thermodynamic interactions between each PI and TAC using a generalized Flory–Huggins interaction parameter, χ. Ignoring entropic contributions, χ can be estimated by

$$\chi = \frac{V_r}{RT}(\delta_1 - \delta_2)^2 \quad (2)$$

where V_r is a reference volume and taken here as the repeat unit molar volume of TAC (215.9 cm^3/mol), R is the universal gas constant, T is temperature, and δ_1 and δ_2 are the solubility parameters of polymer 1 and polymer 2, respectively. The value of the solubility parameter for IN3 has been estimated by Harris et al.[44] using an intrinsic viscosity method as 22.1 $MPa^{1/2}$. We used several group contribution methods to calculate the solubility parameter for IN3 and found that the value of 21.8 $MPa^{1/2}$ calculated by Beerbower's method[45] gave the closest agreement with the value from intrinsic viscosities. Therefore, we also used Beerbower's method to calculate the solubility parameter for IN1 and obtained a value of 23.3 $MPa^{1/2}$. The solubility parameter for TAC depends on its acetyl content, which is 43.6% (according to the manufacturer) for the TAC used in this work. Unfortunately, there are not many experimental values of solubility parameters for TAC with different acetyl contents. Reported values based on group contribution methods range from 18.8 $MPa^{1/2}$ to 31.7 $MPa^{1/2}$.[35,46,47] Mulder et al.[35] reported that the value calculated using the group contribution method developed by van Krevelen agreed fairly well with the experimental value. Here we adopted that contribution method to calculate the solubility parameter for TAC with 43.6% acetyl content and obtained a value of 20.2 $MPa^{1/2}$. Using eq 2 with a segment volume equal to the repeat unit volume of TAC (215.9 cm^3/mol), we obtained χ values of 0.84 for the IN1/TAC pair and 0.22 for the IN3/TAC pair, suggesting that IN1 is much less compatible with TAC, which is consistent with the experimental results for interface width.

Because the interaction parameter χ varies inversely with temperature, we can expect the thermodynamic equilibrium interfacial width between PI and TAC to increase with increasing temperature, but the direct coating process is a nonequilibrium process. The interfacial width formed will depend on diffusion rate, the time available for the polymer molecules to diffuse, and the polymer pair miscibility. The interfacial widths between IN3 and TAC formed under different coating temperatures are plotted in Figure 8, which shows for the temperature range studied a maximum interfacial width value at 35 °C. The adhesion test results in Figure 8 also point to an optimum coating temperature that maximizes the interfacial adhesion in the coating process. To explain the existence of the maximum, we note that there are two key rates to control the interfacial width during the solution casting: the polymer diffusion rate and the solvent evaporation rate. Both the polymer diffusion coefficient, D, and the solvent diffusion rate are increased by raising T. Thus, increasing coating temperature allows more solvent to penetrate into the TAC underlayer, lowering the T_g of TAC within a given time, resulting in more free volume for the polymer molecules to penetrate. Therefore, a faster diffusion of the polymer molecules across the interface is expected at higher temperature. The increase in polymer diffusion rate with increasing

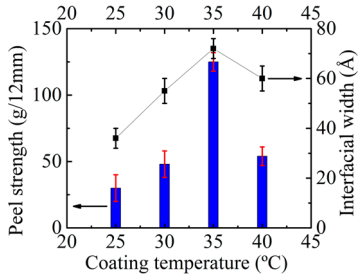

Figure 8. Variations in interfacial width and adhesion with temperature of the IN3/TAC interface prepared by direct casting. Interface widths measured with NR are shown with symbols and read from the right vertical axis (NR data, fits, and SLD profile in the Supporting Information, Figures S17 and S18). Peel strengths shown with solid bars correspond to the left vertical axis. Peel strength increases sharply with increasing interface width in this regime.

temperature would tend to broaden the interface with increasing temperature, all other factors remaining equal.

However, the solvent evaporation rate also increases with increasing coating temperature, which limits the time available for the polymer molecules to diffuse. The final interfacial width is dependent on the balance between these two rates. As illustrated schematically in Figure 9, at lower temperature the

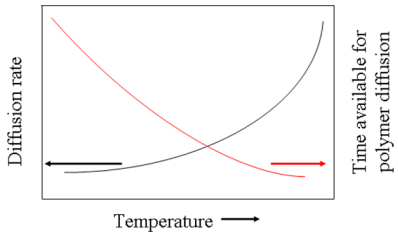

Figure 9. Schematic of the effect of temperature on interdiffusion rate and solvent evaporation rate in the solution-coating process.

low polymer diffusion rate limits the interfacial width. At high temperature, the interfacial width is limited by the diminishing time available to form the interface. The maximum width should be formed at some intermediate temperature, so long as at all these temperatures sufficient thermodynamic driving force exists for mixing across the interface. In fact, there is a third, temperature dependent factor impacting both rates, miscibility. The presence of solvent is not only important to allow polymer mobility, it is also necessary to provide polymer miscibility at the interface. Without the solvent there is little driving force for chains to cross the interface. The effect of the balance of these three factors is the maximum in interface width at an intermediate temperature.

The way in which the interface fails in a peeling should correlate to the interface width and how the interface width affects the mechanism(s) by the interface fails. Further, because the peeling test causes deformation and fracture in the interfacial region, the morphology of the fractured surface should correlate with the peel strength and provide direct information on the history of the fracture and debonding process.[48,49] Figure 10 shows AFM images of the fracture surface of the TAC substrate after peeling tests with the IN3/TAC bilayer films prepared by direct coating of the PI layer on top of the TAC layer using different volume percentages of swelling agent ethyl acetate. The images of the TAC fracture surfaces for 0 vol % and 10 vol % ethyl acetate show similar,

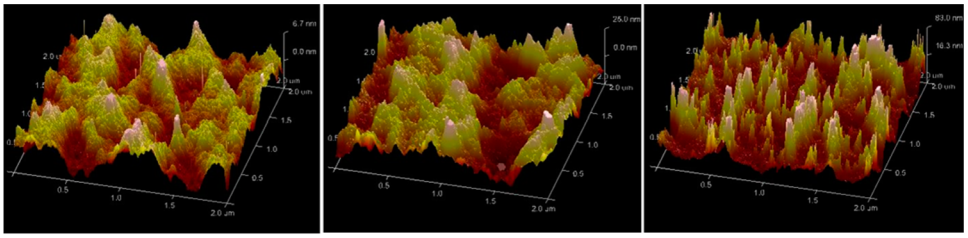

Figure 10. Tapping mode AFM 3-dimensional 2 × 2 μm^2 height images of the fracture surfaces of the TAC layers after peeling tests for IN3/TAC bilayer films prepared by direct solution casting of an IN3 layer on top of a TAC layer using different volume percentages of swelling agent ethyl acetate as marked.

irregular "bumpy" morphologies, whereas the morphology of the TAC fracture surface for 20 vol % ethyl acetate is characterized by a high density of sharp "spikes". Considering the changes in peel strength and AFM images with volume fraction of swelling agent, we conjecture that these sharp "spikes" may be remnants of the connection points between TAC and IN3, i.e., regions where the TAC was substantially deformed upon fracture due to some entanglement across the interface. The higher deformation of the TAC upon fracture for the case of the broader interface is perhaps even more clearly seen by considering cross sections of the AFM topography images shown in Figure 11. For 10 vol % swelling agent there

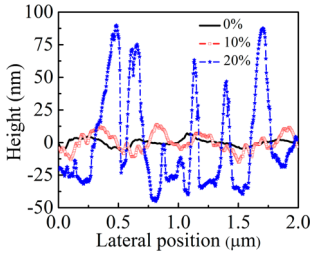

Figure 11. Tapping mode AFM cross-sections of the fracture surfaces shown in Figure 10.

are excursions of the surface ±10 nm about the nominal surface plane, and there is a certain characteristic lateral frequency to these excursions. For 20 vol % swelling agent the excursions are +92/−35 nm and the "spikes" are much narrower than the "bumps" for 10 vol % swelling agent. This significant difference in the magnitude of the surface deformation with changing vol % swelling agent is indicative of a large difference in adhesion at the interface. Our picture of the relationship among the laterally averaged interface width, interface adhesion, and fracture surface morphology is the following. When the interface is quite narrow, only penetration of the chain ends across the interface and into the other polymer is possible. van der Waals forces (vdW) and the force required to pull the chain ends out of the polymer matrix contribute to the measured adhesion forces. The vdW and pullout forces are relatively small. The irregular "bumpy" morphology has been created by the thermal fluctuations present during deposition and perhaps also by inhomogeneous internal stresses in the interfacial region during deposition. As more chain segments diffuse across the interface, interpenetrating chains stitch the two polymer layers together and chain entanglements between the PI and TAC chains are established. If the entanglement density at the interface becomes large enough, chain scission and crazing become the primary fracture mechanisms during peeling tests.[11] In this work, the change in fracture mechanism is evidenced by the sharp change in roughness measured by AFM.

Figure 12 shows the AFM images of the TAC fracture surfaces after peeling tests of IN3/TAC bilayers prepared by

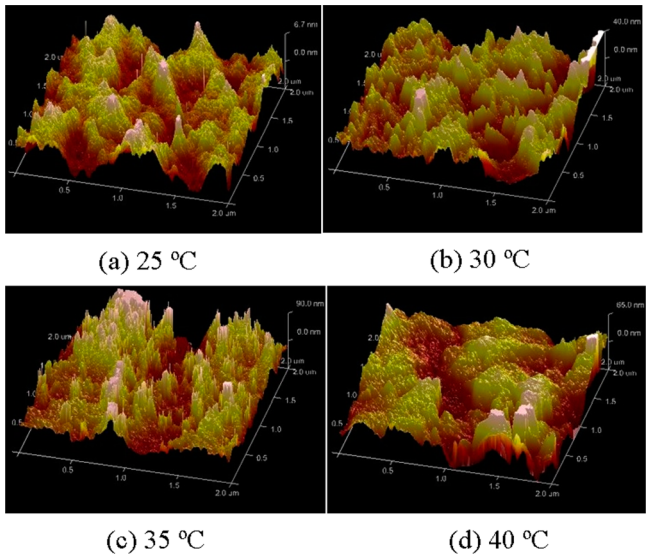

Figure 12. AFM 2 × 2 μm^2 images of the fracture surface of the TAC layer after the peeling test for IN3/TAC bilayer films prepared by direct solution casting of an IN3 layer on top of a TAC layer using different volume percentages of swelling agent ethyl acetate.

direct coating of an IN3 layer on top of a TAC layer at various coating temperatures. Above it was argued that coating temperature affects the interfacial width and adhesion strength between IN3 and TAC as a consequence of changes in the polymer chain diffusion coefficient and the time available for polymer diffusion, with a maximum in interfacial width and peel strength occurring at 35 °C. For the case of increasing peel strength through adding swelling agent, the appearance of "spikes" in the fracture surface morphology is connected with the large increase in peel strength. For the case of changing deposition temperature, the changes in fracture surface morphology that occur when the peel strength goes up are less obvious. The RMS roughness of the fracture surface, plotted in Figure 13, does change with deposition temperature, however. First it increases with deposition temperature, reaches a maximum value at 35 °C, and then slightly decreases with further increase of temperature. However, it appears that adding swelling agent is a much more effective way to increase peel strength. When changing temperature of deposition the

dx.doi.org/10.1021/am3022587 | ACS Appl. Mater. Interfaces 2013, 5, 2976−2984

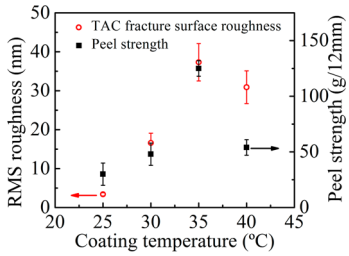

Figure 13. Comparison of the variations with temperature of peel strength and RMS roughness for IN3/TAC bilayer films prepared by direct solution casting. RMS roughnesses of the TAC fracture surface measured with AFM are shown with open circles and read from the left vertical axis. Peel strengths are shown with solid squares and correspond to the right vertical axis.

fracture surface roughness can be increased somewhat more than it is increased by adding swelling agent, but the peel strength is increased only by a factor of 3 by varying temperature, whereas by adding swelling agent an improvement of factor seven can be achieved. We conjecture that this is due to the larger internal stresses created in the interfacial region when deposition is done at higher temperature. It has been shown experimentally that faster solvent evaporation enhances internal stress development.[50] Because the solvent evaporation rate increases rapidly with increasing temperature, we can expect accumulation of higher internal stress in the interface region when coating at higher temperature. This means less force is needed to fracture the interface, so "spikes" indicative of strong deformation of the interface upon peeling are not apparent. The higher roughness for the higher deposition temperature could be due, in part, to larger amplitude fluctuations of the interface at higher temperature that are kinetically trapped upon solvent evaporation.

4. CONCLUSIONS

NR measurements reveal that the interface formed between a layer of organo-soluble rigid-rod-like aromatic polyimide and a TAC layer by spin-coating or solution-casting of the PI layer directly on top of the TAC layer has a laterally averaged, effective width of less than 4 nm fwhm, explaining the poor interlayer adhesion for this case. The width of the interface between IN3 and TAC, and thereby the interlayer adhesion, can be controlled to some extent by adding the swelling agent ethyl acetate, a poor solvent for TAC, to the PI solution being cast upon the TAC layer. The interlayer adhesion, as measured by T-peel tests, can be improved by up to a factor of 7 in this way. In the case of IN1, a PI with even poorer miscibility with TAC, use of the poor solvent swelling agent strategy does not provide noticeable improvement in adhesion. Use of the swelling agent to improve the interface adhesion is only effective when thermodynamic interactions between the PI and TAC layers are not too unfavorable. Since there exists a competition between the interlayer polymer diffusion and solvent evaporation, there exists an optimum temperature to maximize interface width and adhesion, but adding swelling agent appears to be a more effective means of enhancing interfacial adhesion.

The prerequisites for a solvent to serve as a good swelling agent may be generalized. The ethyl acetate acts as a swelling agent because the lower polymer layer has some limited solubility in it. The solubility of the lower polymer in the swelling agent must be large enough that the material at the surface of the underlying polymer imbibes some of the swelling agent, but not so much that the surface of the underlying polymer is dissolved in the swelling agent and therefore badly disrupted. The swelling agent must also be miscible with the casting solvent for the upper layer. When only a limited concentration of swelling agent is absorbed in the near surface region of the lower polymer layer, both the mobility of those chains and their mutual solubility with the polymers in the top layer are enhanced temporarily. The near surface layer of the underlying polymer swells because of a modest entropy gain by mixing. Thus the key chemical prerequisites for the swelling agent are the right degrees of similarity to the chemistries of the underlying polymer and the casting solvent. The volatility of the swelling agent is a second consideration. The swelling agent should not be very volatile so that the TAC surface layer can remain in a mobile state long enough to allow sufficient interdiffusion of TAC molecules across the interface. On the other hand, the swelling agent must also not be too difficult to remove during drying.

■ ASSOCIATED CONTENT

Supporting Information

DSC data, neutron reflectivity data and fits, and SLD profiles. This material is available free of charge via the Internet at http://pubs.acs.org.

■ AUTHOR INFORMATION

Corresponding Author

*E-mail: mfoster@uakron.edu.

Present Address

⊥B.A. is currently at Department of Chemistry, Bogazici University, Bebek 34342, Istanbul, Turkey

Notes

The authors declare no competing financial interest.

■ ACKNOWLEDGMENTS

Research support from a Wright Center of Innovation Grant and DURIP grants W911NF-09-1-0122 and W911NF-10-1-0167. We acknowledge support of the National Institute of Standards and Technology, U.S. Department of Commerce, in providing the neutron research facilities used in this work. Commercial materials, instruments and equipment are identified in this paper in order to specify the experimental procedure as completely as possible. In no case does such identification imply a recommendation or endorsement by the National Institute of Standards and Technology nor does it imply that the materials, instruments, or equipment identified are necessarily best available for the purpose.

■ REFERENCES

(1) Harris, F. W.; Sun, L.; Zhang, D.; Cheng, S. Z. D. U.S. Pat. Appl. Publ. U.S. 2009 0 197 019, August 6, 2009.
(2) Moran, D.; Whitmore, P. M. *Mater. Res. Soc. Symp. Proc.* **1995**, *352*, 293−303.
(3) Francis, L. F.; McCormick, A. V.; Vaessen, D. M.; Payne, J. A. *J. Mater. Sci.* **2002**, *37*, 4717−4731.
(4) Wool, R. P. *Polymer Interfaces: Structure and Strength*; Hanser Publishers: New York, 1995; pp 41−60.
(5) Wu, S. *Polymer Interface and Adhesion*; Marcel Dekker: New York, 1982, pp 1−28.
(6) Fernandez, M. L.; Higgins, J. S.; Penfold, J.; Shackleton, C.; Walsh, D. J. *Polymer* **1990**, *31*, 2146−2151.
(7) Stamm, M. *Adv. Polym. Sci.* **1992**, *100*, 357−400.

(8) Schnell, R.; Stamm, M.; Creton, C. *Macromolecules* **1998**, *31*, 2284−2292.
(9) Brown, H. R. *Macromolecules* **2001**, *34*, 3720−3724.
(10) Creton, C.; Kramer, E.; Brown, H. R.; Hui, C. *Adv. Polym. Sci.* **2002**, *156*, 53−136.
(11) Cole, P. J.; Cook, R. F.; Macosko, C. W. *Macromolecules* **2003**, *36*, 2808−2815.
(12) Silvestri, L.; Brown, H. R.; Carrà, S.; Carrà, S. *J. Chem. Phys.* **2003**, *119*, 8140−8149.
(13) Marosi, G.; Bertalan, G. In *Modification and Blending of Synthetic and Natural Macromolecules*; Ciardelli, F., Penczek, S., Eds.; Kluwer Academic Publishers: Dordrecht, The Netherlands, 2004; pp 135−154.
(14) Harada, M.; Suzuki, T.; Ohya, M.; Kawaguchi, D.; Takano, A.; Matsushita, Y.; Torikai, N. *J. Polym. Sci., Part B: Polym. Phys.* **2005**, *43*, 1486−1494.
(15) Schach, R.; Tran, Y.; Menelle, A.; Creton, C. *Macromolecules* **2007**, *40*, 6325−6332.
(16) Busch, P.; Weidisch, R. In *Polymer Surfaces and Interfaces: Characterization, Modification and Applications*; Stamm, M., Ed.; Springer-Verlag: New York, 2008; pp 161−182.
(17) Helfand, E. *J. Chem. Phys.* **1972**, *56*, 3592−3601.
(18) Helfand, E.; Tagami, Y. *J. Chem. Phys.* **1972**, *57*, 1812−1813.
(19) Broseta, D.; Fredrickson, G. H.; Helfand, E.; Leibler, L. *Macromolecules* **1990**, *23*, 132−139.
(20) Li, F.; Harris, F. W.; Cheng, S. Z. D. *Polymer* **1996**, *37*, 5321−5325.
(21) Cheng, S. Z. D.; Wu, Z.; Mark, E.; Hsu, S. L. C.; Harris, F. W. *Polymer* **1991**, *32*, 1803−1810.
(22) Matsuura, T.; Hasuda, Y.; Nishi, S.; Yamada, N. *Macromolecules* **1991**, *24*, 5001−5005.
(23) Harris, F. W.; Cheng, S. Z. D. U.S. Patent 5 480 964, January 2, 1996.
(24) Choi, M.; Kim, Y.; Ha, C. *Prog. Polym. Sci.* **2008**, *33*, 581−630.
(25) Chao, Y.; Huang, S.; Chen, C.; Chang, Y.; Meng, H.; Yen, F.; Lin, I.; Zan, H.; Horng, S. *Synth. Met.* **2011**, *161*, 148−152.
(26) Dupont, S. R.; Oliver, M.; Krebs, F. C.; Dauskardt, R. H. *Sol. Energy Mater. Sol. Cells* **2012**, *97*, 171−175.
(27) Russell, T. P. *Mater. Sci. Rep.* **1990**, *5*, 171−271.
(28) Roe, R. J. *Methods of X-ray and Neutron Scattering in Polymer Science*; Oxford University Press: New York, 2000; pp236−260.
(29) Harris, F. W. In *Polyimides*, Wilson, D., Stenzenberger, H. D., Hergenrother, P. M., Eds.; Blackie and Son: New York, 1990; pp 1−35.
(30) Li, F.; Kim, K.; Kulig, J. J.; Savitski, E. P.; Brittain, W. J.; Harris, F. W.; Cheng, S. Z. D.; Hubbard, S. F.; Singer, K. D. *J. Mater. Chem.* **1995**, *5*, 353−359.
(31) Piranha etching consists of using hydrogen peroxide and sulfuric acid, which can be dangerous. Acid-resistant gloves, protective goggles, and lab coats must be worn when handling the piranha solution.
(32) Jones, R. A. L.; Richards, R. W. *Polymers at Surfaces and Interfaces*; Cambridge University Press: Cambridge, U.K., 1999; pp 127−186.
(33) Kienzle, P. A.; O'Donovan, K. V.; Ankner, J. F.; Berk, N. F.; Majkrzak, C. F. http://www.ncnr.nist.gov/reflpak. 2000−2006 (accessed May 13, 2012).
(34) Omatete, O. O.; Bodaghi, H.; Fellers, J. F.; Browne, C. L. *J. Rheol.* **1986**, *30*, 629−659.
(35) Mulder, M. H. V.; Kruitz, F.; Smolders, C. A. *J. Membr. Sci.* **1982**, *11*, 349−363.
(36) Dai, K. H.; Norton, L. J.; Kramer, E. J. *Macromolecules* **1994**, *27*, 1949−1956.
(37) Sferrazza, M.; Xiao, C.; Jones, R. A. L.; Bucknall, D. G.; Webster, J.; Penfold, J. *Phys. Rev. Lett.* **1997**, *78*, 3693−3696.
(38) Sferrazza, M.; Jones, R. A. L.; Penfold, J.; Bucknall, D. B.; Webster, J. R. P. *J. Mater. Sci.* **2000**, *10*, 127−132.
(39) Fujii, Y.; Atarashi, H.; Hino, M.; Nagamura, T.; Tanaka, K. *ACS Appl. Mater. Interfaces* **2009**, *1*, 1856−1859.
(40) Tanaka, K.; Fujii, Y.; Atarashi, H.; Akabori, K.; Hino, M.; Nagamura, T. *Langmuir* **2008**, *24*, 296−301.
(41) Asmussen, F.; Ueberreiter, K. *J. Polym. Sci.* **1962**, *57*, 199−208.
(42) Ueberreiter, K.; Asmussen, F. *J. Polym. Sci.* **1962**, *57*, 187−198.
(43) Ueberreiter, K. In *Diffusion in Polymers*; Crand, J., Park, G. S., Eds; Academic Press: New York, 1968; pp 219−257.
(44) Harris, F. W.; Li, F.; Cheng, S. Z. D. In *Fluoropolymers: Properties*; Hougham, G., Cassidy, P. E., Johns, K., Davidson, T., Eds.; Kluwer Academic: New York, 1999; pp 351−370.
(45) Hansen, C. M. *Hansen Solubility Parameters: a User's Handbook*, 2nd ed.; CRC Press: New York, 2007; pp 1−26.
(46) Mandal, S.; Pangarkar, V. G. *J. Membr. Sci.* **2002**, *201*, 175−190.
(47) Ong, R. C.; Chung, T. S. *J. Membr. Sci.* **2012**, *394*−*395*, 230−240.
(48) Zhong, Q.; Inniss, D.; Kjoller, K.; Elings, V. B. *Surf. Sci.* **1993**, *290*, L688−L692.
(49) Wetzel, B.; Rosso, P.; Haupert, F.; Friedrich, K. *Eng. Fract. Mech.* **2006**, *73*, 2375−2398.
(50) Perera, D. Y. In *Plastics and Coatings: Durability, Stabilization, Testing*; Ryntz, R. A., Ed.; Hanser: Munich, 2001; pp 115−139.